Notes

Effect of Particle Size, Composition, and Thermal Treatment on the Crystalline Structure of Polycaprolactone Nanoparticles

Eun Chul Cho,*,† Kilwon Cho,‡ Jong Kun Ahn,§ Junoh Kim,† and Ih-Seop Chang†

Skin Research Institute, Amorepacific Corporation/ R&D Center, 314-1, Bora-dong, Giheung-gu, Yongin, 446-729, Korea, Department of Chemical Engineering, Polymer Research Institute, Pohang University of Science and Technology, Pohang, 790-784, Korea, and Department of Agricultural Science, Korea National Open University, 169 Dongsoong-dong, Chongno-gu, Seoul, 110-791, Korea

Received November 21, 2005
Revised Manuscript Received February 26, 2006

Introduction

Biodegradable, biocompatible nanoparticles have been used in various fields, such as drug delivery systems,[1] cosmetics,[2] and tissue engineering.[3] For such applications, these nanoparticles are usually loaded with water-insoluble drugs. Thus, it is imperative that the internal structure of the nanoparticles is known, since specific drug amounts loaded into the nanoparticles and particular drug release patterns are not only dependent on the hydrophilicity of the drug but also on the internal structure of the nanoparticles.

The internal structure of polymeric particles can be influenced by the various characteristics of the polymer, such as chemical structure,[4] molecular geometry,[5] molecular weight,[6] and crystalline structure.[7] Generally, the structures of micro/nanoparticles are determined either by analyzing dried (lyophilized) particles[7,8] or deduced from the properties of the bulk materials.[9] However, most in vitro/vivo experiments are carried out in aqueous systems, and hence, it would be more desirable to determine the structure in an aqueous environment rather than in the dried state. Such a requirement is more urgent for polymeric nanoparticles because an anticoagulant agent (i.e. Pluronic) or a hydrophilic part of a nanoparticle (i.e. poly(ethylene oxide)) in a dried state might mislead by yielding a different structure for the nanoparticles. Therefore, it is necessary to find a tool to accurately characterize the structure of the nanoparticles in the dispersion state. Recently, Bunjes et al. studied aqueous dispersions of triglyceride nanoparticles using calorimetry and X-ray scattering and showed that the internal structure of a nanoparticle depends on its size.[10] Castelli et al. conducted a similar characterization study of solid lipid nanoparticles using differential scanning calorimetry.[11]

In this work, we prepared two types of nanoparticles, polycaprolactone (PCL) homopolymer and PCL/PCL-*b*-poly(ethylene oxide) (PEO) nanoparticles, and conducted a structural analysis of these nanoparticles using microcalorimetry and transmission electron microscopy (TEM). The objectives of such analysis are to demonstrate how the structure of these nanoparticles is affected by particle size, thermal treatment, and the composition of the homopolymer to block copolymer ratio.

Experimental Section

In this study, nanoparticles were prepared from (1) a PCL homopolymer and (2) a PCL/PCL-*b*-PEO having a PCL molecular weight of block copolymer similar to that of the PCL homopolymer. Nanoparticle sizes were controlled by varying both the polymer concentration in an organic solvent and the homopolymer to block copolymer ratio.

Materials and Synthesis of Block Copolymer. Polycaprolactone ($M_n \sim 10$ K) was obtained from Aldrich, while the poly(ethylene glycol)-*b*-poly(propylene glycol)-poly(ethylene glycol) (PEO-*b*-PPO-*b*-PEO) (Pluronic F68) triblock copolymer was obtained from BASF. PCL-*b*-PEO was synthesized by bulk ring opening polymerization. Methoxylated PEG ($M_n \sim 5000$, Fluka) was first vacuum-dried at 110 °C with continuous stirring for 3 h and then cooled to room temperature. Following the addition of stannous hexanoate (Aldrich) and ϵ-caprolactone (Aldrich), this mixture was then vacuum-dried for 3 h at room temperature before polymerization at 130 °C over a 24-h period. Subsequently, the reactant was solubilized in tetrahydrofuran (THF) and transferred into an excess amount of diethyl ether. This purification process was repeated twice. The resulting M_n value calculated from NMR spectra is in good agreement with the value obtained by GPC ($M_n \sim 14\,000$ and $M_w/M_n \sim 1.1$), which was calibrated against a polystyrene standard in THF.

Preparation of PCL and PCL/PCL-*b*-PEO Nanoparticles. PCL homopolymer nanoparticles were prepared as follows. The appropriate quantity of PCL was solubilized in 67 mL of acetone, and this solution was transferred into 100 mL of a 0.17 wt % Pluronic F68 aqueous solution with continuous stirring at room temperature. After 5 min, the acetone was removed by vacuum evaporation at 30 °C. The size of the PCL nanoparticles was controlled by varying the concentration of PCL in acetone to 1.49, 10, and 20 mg/mL. The final concentration of the three PCL homopolymer nanoparticles was 1.3 wt % in Pluronic F68 aqueous solution.

The PCL/PCL-*b*-PEO nanoparticles were prepared via the same method as the PCL nanoparticles. Known quantities of PCL and PCL-*b*-PEO (with a combined total weight of 2 g) were solubilized in 67 mL of acetone, and the solution was transferred into 100 mL of distilled water with continuous stirring at room temperature. The acetone was removed by vacuum evaporation at 30 °C. The nanoparticle sizes were controlled by varying the weight ratio of PCL to PCL-*b*-PEO; the ratios used were 20, 3, 1, 0.33, and 0 (no PCL present). The final concentration of the five nanoparticle aqueous solutions was 4 wt %.

Measurement of Nanoparticle Size. The nanoparticle size and distribution was determined using photon correlation spectroscopy (PCS, Malvern Instrument 4500HS); the principle underlying this approach is well documented.[12] The aqueous nanoparticle dispersions were diluted to 0.1 mg/mL, and the intensity of the He−Ne laser light (633 nm) scattered by the samples was detected at an angle of 90°. For each specimen, 10 autocorrelation functions were analyzed using the scattered intensity and the mean diameter of the nanoparticles calculated using the Stokes−Einstein equation. The size distribution was calculated using the CONTIN routine.

Thermal Analysis of Nanoparticles. The PCL and PCL/PCL-*b*-PEO nanoparticle structures were analyzed using microcalorimetry (VP-DSC, MicroCal). Microcalorimetry has been very useful in measuring

* To whom correspondence should be addressed. E-mail: enjo@amorepacific.com.
† Amorepacific Corporation/R&D Center.
‡ Pohang University of Science and Technology.
§ Korea National Open University.

10.1021/bm050883s CCC: $33.50
Published on Web 04/04/2006

the thermal properties of aqueous dispersions, such as synthetic polymers,[13] proteins,[14] and nanoparticle aqueous solutions.[10,11] Equal volumes (0.5 mL) of an aqueous nanoparticle dispersion and reference solution were injected into the sample and reference cells, respectively. The cells were then closed tightly (≈25−30 psi) so that water could not distill out during the experiment. The nanoparticle dispersions were thermally equilibrated to 5 °C and scanned from 5 to 80 °C, with a scanning rate of 1 °C/min. During each scan, the heat capacity difference between the sample cell and the reference cell was plotted as a function of temperature. Since the PCL nanoparticles were dispersed in Pluronic F68 solution, the reference cell was also filled with Pluronic F68 aqueous solution (without nanoparticles) of the same concentration. The PCL/PCL-*b*-PEO nanoparticles, on the other hand, were dispersed in water, and so deionized water was used as the reference solution. To compare the microcalorimetry thermograms with those obtained by conventional DSC, nanoparticle solutions of the same concentration were also analyzed using differential scanning calorimetry (DSC Q1000, TA Instrument). The scanning rate and scan temperature range were equal to those used in the microcalorimetry studies. To prevent the evaporation of water in the nanoparticle solution and to stabilize the baseline, a high volume pan was used and He gas (50 mL/min) was purged through the system during each scan.

TEM Studies on PCL/PCL-*b*-PEO Nanoparticles. The structure of the PCL/PCL-*b*-PEO nanoparticles was observed using transmission electron microscopy (TEM, Hitachi H-7600). The nanoparticle solutions were stained with a 20 wt % aqueous solution of phosphotungstic acid, and the stained solutions were floated on gold-coated EM grids. These grids were immediately freeze-dried with liquid nitrogen and then lyophilized with a freeze-drier.

Results and Discussion

Effect of Nanoparticle Size on the Crystalline Structure of PCL Homopolymer Nanoparticles. Generally, polymeric nanoparticles are prepared via one of two methods: solvent evaporation[15] or the solvent displacement method.[16] When using a water miscible solvent such as acetone, THF, or ethanol, the solvent displacement method is usually the most useful in preparing nanoparticles. The main factor in controlling the size of the nanoparticle is reported to be the concentration of the polymer in the organic solvent.[16] Therefore, the PCL concentration in acetone was varied (1.49, 10, and 20 mg/mL) to produce PCL nanoparticles of different sizes. Figure 1a−c shows histograms of the size distribution of the as-formed PCL nanoparticles. In general, the particle size was found to increase as the PCL concentration increased; however, the particle size did not change significantly in the concentration region between 10 and 1.49 mg/mL, as shown in Figure 1d. Furthermore, below a concentration of 1.49 mg/mL, it was not possible to reproducibly generate nanoparticles of a particular size (average sizes ranged from 200 to 100 nm for a certain concentration). A certain quantity of surfactant can be added to prepare the smaller nanoparticles; however, this method is inappropriate for the present work because the surfactant could affect the structure of the PCL nanoparticles.

Before reporting on the structure of the PCL nanoparticles, it is first necessary to investigate the thermal properties of the bulk PCL. Figure 2a shows the DSC thermograms (TA DSC, 1 °C/min from 0 to 80 °C) of the PCL homopolymer ($M_n \sim 10$ K). A single endothermic peak around 60 °C in the first scan could be resolved into two peaks following cooling and reheating (second scan). Further, the single peak in the first scan is shifted to a lower temperature after rescanning, indicating that different crystalline structures (i.e. different lamella orientations and fold numbers) exist after the melting and cooling processes. In addition, PCL has a slight higher crystallinity after

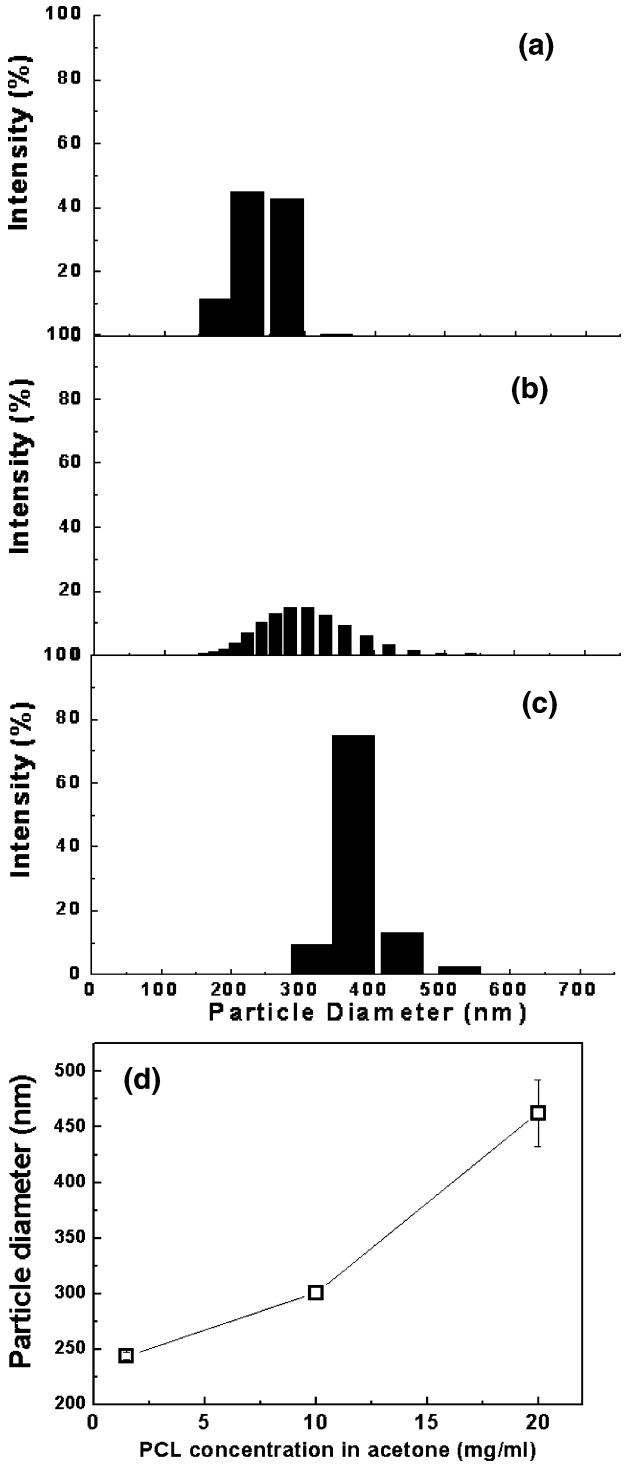

Figure 1. Size distribution histograms of the PCL nanoparticles as a function of preparation concentration: (a) 1.49 mg/mL; (b) 10 mg/mL; (c) 20 mg/mL. Average diameters of the PCL nanoparticles are plotted in (d).

the melting and cooling processes, when comparing the heat of fusion of the melting peak for the first (90.7 J/g) and second (95.6 J/g) scans. It is reported that wide-angle X-ray scattering shows that PCL has an orthorhombic crystalline structure with (110) and (200) planes[17,18] and that the double melting point is due to the presence of crystalline lamellae with different fold numbers.[19] The two endothermic peaks in the PCL thermogram might therefore originate from the different orientations of this orthorhombic crystalline structure and from crystalline lamellae with different fold numbers.

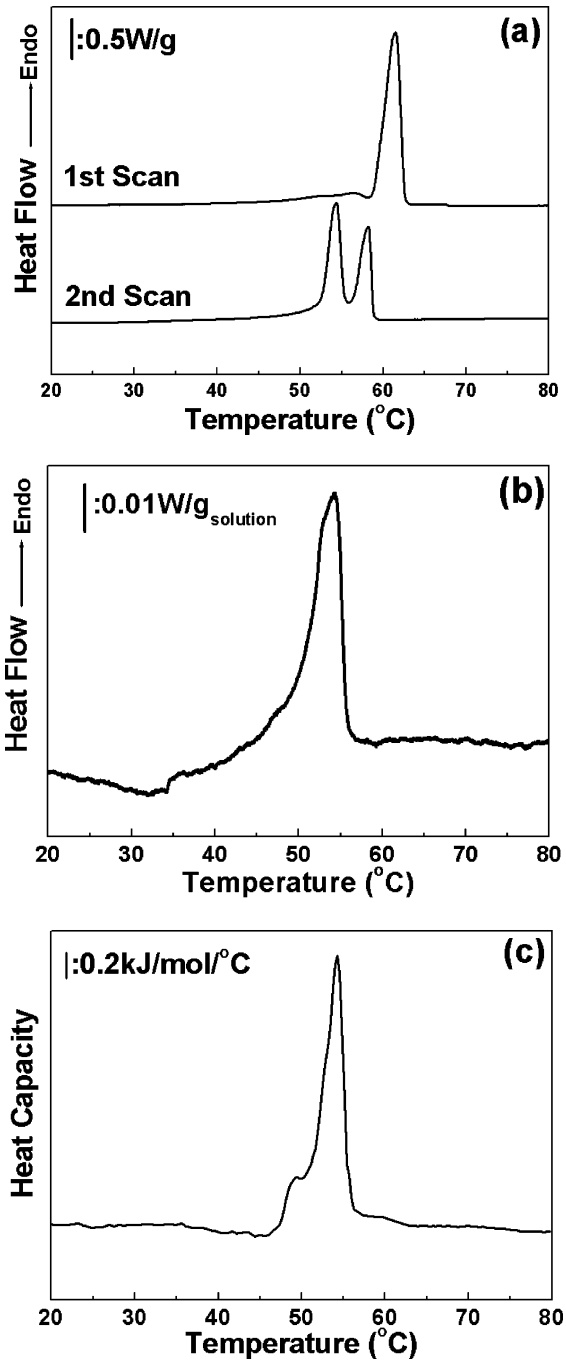

Figure 2. Thermograms of PCL and PCL nanoparticle aqueous solutions: (a) PCL in the bulk determined using conventional DSC; (b) PCL nanoparticle aqueous solution determined using conventional DSC; (c) PCL nanoparticle aqueous solution determined using microcalorimetry. The average particle diameter is 301 nm and nanoparticle concentration is 1.3 wt %.

The thermograms of the first scan for the PCL nanoparticle solutions (average diameter of 301 nm) are shown in Figure 2b (TA DSC) and Figure 2c (microcalorimetry). A single endothermic peak was detected in both thermograms at 54.4 °C (in Figure 3, it can be shown that this peak corresponds to the right-side peak of bulk PCL), where the peak position is ~4 °C lower than that of the bulk PCL (as determined by a second scan of bulk PCL). From these thermograms, it can be said that the lower peak temperature of the PCL nanoparticles (as compared to that of the bulk PCL) is due to the difference between the structures of bulk PCL and the PCL nanoparticles rather than from the use of different analytical instruments. Although the

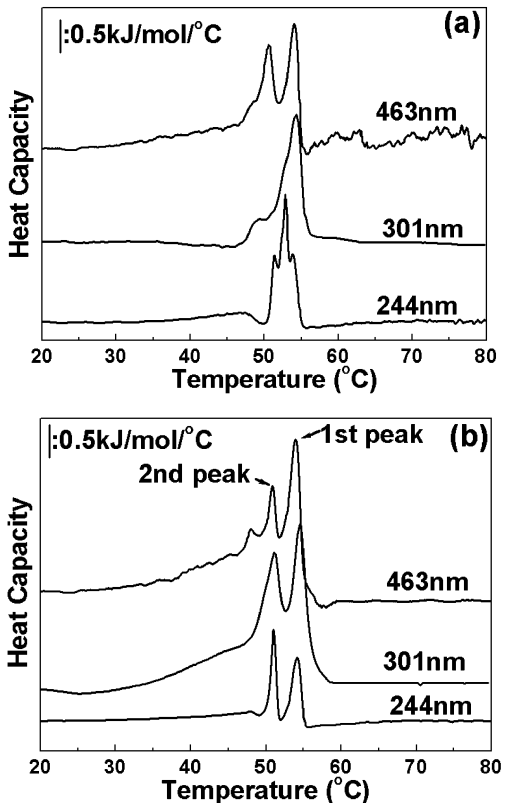

Figure 3. Microcalorimetry thermograms for PCL nanoparticle solutions with different particle diameters: (a) first scan from 5 to 80 °C; (b) second scan from 5 to 80 °C after cooling from 80 to 5 °C.

two instruments recorded similar thermograms for the PCL nanoparticles, it is likely that a notable amount of water in the nanoparticle solution was distilled out when using TA DSC, because a baseline drift was detected in some cases. Therefore, we believe that microcalorimetry can provide more accurate structural information about nanoparticles in solution.

Microcalorimetry samples of three PCL nanoparticle solutions (particle sizes of 244, 301, and 463 nm) were scanned from 5 to 80 °C with a scan rate of 1 °C/min. After the first scan, the solutions were cooled to 5 °C and then rescanned from 5 to 80 °C at the same scan rate (second scan). The corresponding microcalorimetry thermograms for the first and second scans are shown in Figure 3a,b, respectively. The largest of the three nanoparticles (463 nm) exhibited two separate peaks in the first scan; however, these two peaks were not clearly developed for nanoparticles of 244 and 301 nm. On the other hand, two separate peaks were clearly observed in the second scans of all three nanoparticle solutions (Figure 3b). A third scan (data not shown) for the three particle solutions, however, showed no peak shift or further peak separation from those seen in Figure 3b.

The above results demonstrate that the crystalline structure of the nanoparticles is influenced by both particle size and thermal history. From Figure 3, it can be seen that the larger nanoparticles (463 nm) reach the two crystalline forms faster than the smaller particles. However, thermal treatment enables the smaller particles to have the same two crystalline structures as the large particles.

For the smaller PCL nanoparticles, despite observing different thermograms after the second scan, the size of the PCL nanoparticles was not observed to change. Following the second scan, the nanoparticle solutions were removed from the microcalorimetry cell and the diameters measured using PCS. The

Table 1. Thermal Analysis of the Bulk PCL and PCL Homopolymer Nanoparticles

	peak temp (°C)			
	first scan		second scan	
sample	first peak[a]	second peak	first peak	second peak
bulk PCL 10 K	61.5	ND[b]	58.2	54.4
PCL 10 K, 463 nm	54.1	50.6	53.9	50.9
PCL 10 K, 301 nm	54.4	ND[b]	54.5	51.0
PCL 10 K, 244 nm	53.8	51.4[c]	54.2	51.0

[a] The first and second peaks are assigned in Figure 3b. [b] ND = not detected; shoulder around 50 °C was detected for the PCL particles of 301 nm. [c] Peak was not clearly separated for the PCL particles of 244 nm, as shown in Figure 3a.

results indicated that the PCL nanoparticles have the same hydrodynamic diameters before and after the experiment within experimental errors. It is expected that the smaller PCL nanoparticles (244 and 301 nm) have different diameters before and after the microcalorimetry experiment, because the crystalline structure of these particles has changed (Figure 3). To clarify these results, the three PCL nanoparticle sizes (244, 301, and 463 nm) were annealed at different temperatures (40, 50, and 60 °C, respectively) over a 24-h period, and the sizes of the resulting nanoparticles were measured using PCS. Similar size measurements were also performed for as-prepared nanoparticles at the same three annealing temperatures. On the basis of these results, it is thought that the crystalline structure of the PCL nanoparticles (244 and 301 nm) changed while the particle diameter remained the same. However, it was not possible to exclude the possibility that the PCS study could not discriminate between the changes in particle size with changing crystalline structure. As such, a further study using X-ray scattering should be carried out to clearly explain the relationship between particle diameter and structure change due to annealing of these particles.

Table 1 summarizes the peak temperatures of the bulk PCL and PCL nanoparticles. In a comparison of the corresponding second scan peaks of the PCL nanoparticles and bulk PCL, it is shown that the first and second peak temperatures of the PCL nanoparticles decreased to ~4 °C (first peak) and ~3 °C (second peak), respectively. Similar decreases in melting temperature have been reported for the crystalline nanoparticles. Westesen and Bunjes compared the melting temperatures of solid lipid nanoparticles with the bulk lipid and reported that the melting temperature of the triglyceride nanoparticles decreased to ≈3−5 °C compared to the bulk triglyceride.[20] Westesen et al. also found in their X-ray diffraction studies that the crystalline structure of the solid lipid nanoparticles was different from that of the bulk lipid.[21] In addition, Bunjes et al. recently reported that the melting temperature of the triglyceride nanoparticles of size 365 nm decreased to ≈2−3 °C, as compared to the bulk triglyceride.[10] The aforementioned reports indicate that the solid lipid nanoparticle melting temperature decreased due to differences in crystalline structure between the nanoparticles and the bulk material.

It is worth noting from the results in Figure 3 and Table 1 that the melting temperatures of the three PCL nanoparticles are almost the same regardless of the particle size. There are a few reports on the size-dependent melting temperature and structural changes of the crystalline nanoparticles.[10,20,22] Westesen and Bunjes reported that the melting temperature of the solid lipid nanoparticles did not change for particle sizes between 140 and 60 nm.[20] In contrast, recent reports by Bunjes et al. showed that the triglyceride nanoparticles became lowered in the melting temperature as the particle diameter decreased.[10] In addition, the single endothermic peak associated with the larger nanoparticles was split into small multiple peaks. The corresponding X-ray scattering results suggested that this phenomenon was due to a change in the crystalline and multilayer structure of the triglyceride. In a simulation study, Fukui et al. found that the melting and glass transition temperatures of semicrystalline nanoparticles decrease as the particle diameter decreases.[22] For example, as calculated from their linear relationship, the melting temperature of polyethylene (PE) nanoparticles decreases linearly such that when the particle diameter reaches ~40 nm, the melting temperature is equal to that of bulk PE.

The melting temperature depression can be also observed for the crystalline polymer thin films. Wang et al.[23] showed that the melting temperature of ethylene vinyl acetate (EVA) copolymer films starts to drop significantly when the film thickness falls below ~200 nm. For low-density polyethylene, the melting temperature drops when the thickness is below 150 nm. Wang et al. also commented that the melting point depression of thin films could be a function of both film thickness and the interaction with the substrate.

The results of the above studies suggest that, in the current experiment, the PCL nanoparticles with sizes 463, 301, and 244 nm may be too large to observe the changes in melting temperature. To establish whether the melting temperature of the PCL nanoparticles changes with particle size, a further decrease in nanoparticle size is required.

Effect of Nanoparticle Size on the Crystalline Structure of PCL/PCL-*b*-PEO Nanoparticles. Past results[10,20,22,23] suggest that a further reduction in nanoparticle size is needed to investigate the size-dependent structural change of the nanoparticles in more detail. For this purpose, nanoparticles composed of a PCL homopolymer (10 K) and PCL(9 K)-*b*-PEO(5 K) block copolymer were prepared, where the PCL component in both the homopolymer and block copolymer is assumed to participate in the crystal formation inside the nanoparticle core. Another objective for the preparation of mixed PCL/PCL-*b*-PEO nanoparticles is to investigate the structural differences between the homopolymer nanoparticles and homopolymer/copolymer nanoparticles. Since the PEO chains in the block copolymer stabilize the nanoparticles in water, Pluronic F68 was not necessary for the preparation of these nanoparticles. The nanoparticle size was reproducibly controlled from 62 to 255 nm by adjusting the homopolymer to block copolymer ratio (see Figure 4), where nanoparticles of certain sizes were symmetrically distributed from the most probable point.

The microcalorimetry thermograms and thermal properties of the aqueous dispersions of PCL/PCL-*b*-PEO nanoparticles are shown in Figure 5 and Table 2, respectively. As shown in Figure 5a,b, the melting temperature of the nanoparticles did not change with decreasing particle size (255, 206, and 155 nm). The main melting temperature is around 54 °C, which is the same temperature as that observed for the PCL homopolymer nanoparticles. In addition, the heat capacity difference (ΔC_p) between C_p of the peak around 54 °C and C_p of the baseline at the peak temperature was found to decrease as the nanoparticle size decreased. Furthermore, the nanoparticles with sizes 104 and 62 nm did not show a melting temperature peak during the first and second scans (Figure 5c).

It seems from the results in Figure 5 and Table 2 that ΔC_p decreased as the nanoparticle size decreased. However, it can also be said that the increase in the block copolymer caused ΔC_p to decrease. Therefore, before we discuss the size-dependent decrease in ΔC_p, it is worth investigating whether this decrease in ΔC_p is due to a reduction in the total amount of PCL in the small nanoparticles. Here, the experimental ΔC_p

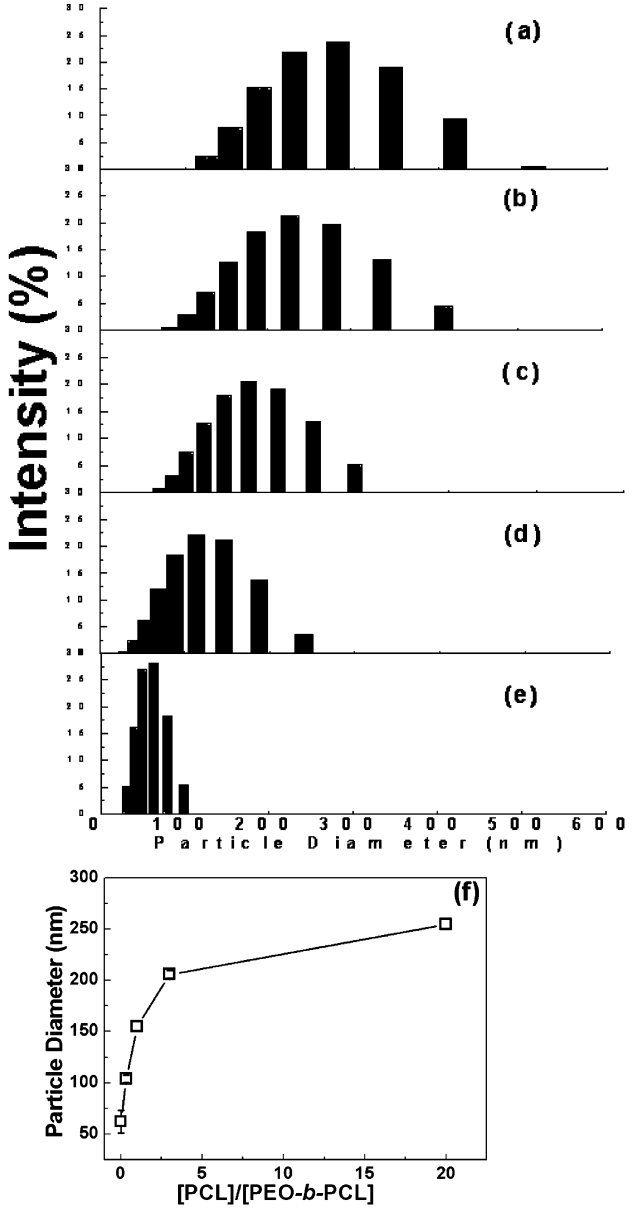

Figure 4. Size distribution histograms of the PCL/PCL-*b*-PEO nanoparticles for different homopolymer to block copolymer ratios: (a) 20; (b) 3; (c) 1; (d) 0.33; (e) 0. Average diameters of the PCL/PCL-*b*-PEO nanoparticles are plotted in (f).

values for two of the smaller PCL/PCL-*b*-PEO nanoparticles (206 and 155 nm) are 0.40 and 0.39 kJ/(mol/°C) (first scan), and 0.30 and 0.28 kJ/(mol/°C) (second scan), respectively. When one calculates ΔC_p on the basis of the relative PCL content in the nanoparticles (i.e., compared to ΔC_p for the 255 nm sized particles), the estimated ΔC_p is determined to be 1.26 kJ/(mol/°C) (88.3% of PCL relative to 255 nm) and 1.13 kJ/(mol/°C) (79.6% of PCL) for the first scan and 0.93 and 0.84 kJ/(mol/°C) for the second scan.

The difference between the experimental and calculated values indicates that other factors besides the decrease in the total amount of PCL in the nanoparticles are involved in the decrease of ΔC_p. One possible scenario for the large drop in ΔC_p is that the reduction in particle size causes the crystalline core of PCL to become disordered. This idea is supported by Bunjes et al., who reported that both the peak temperature and the heat of fusion of triglyceride nanoparticles decreased with decreasing nanoparticle size.[10]

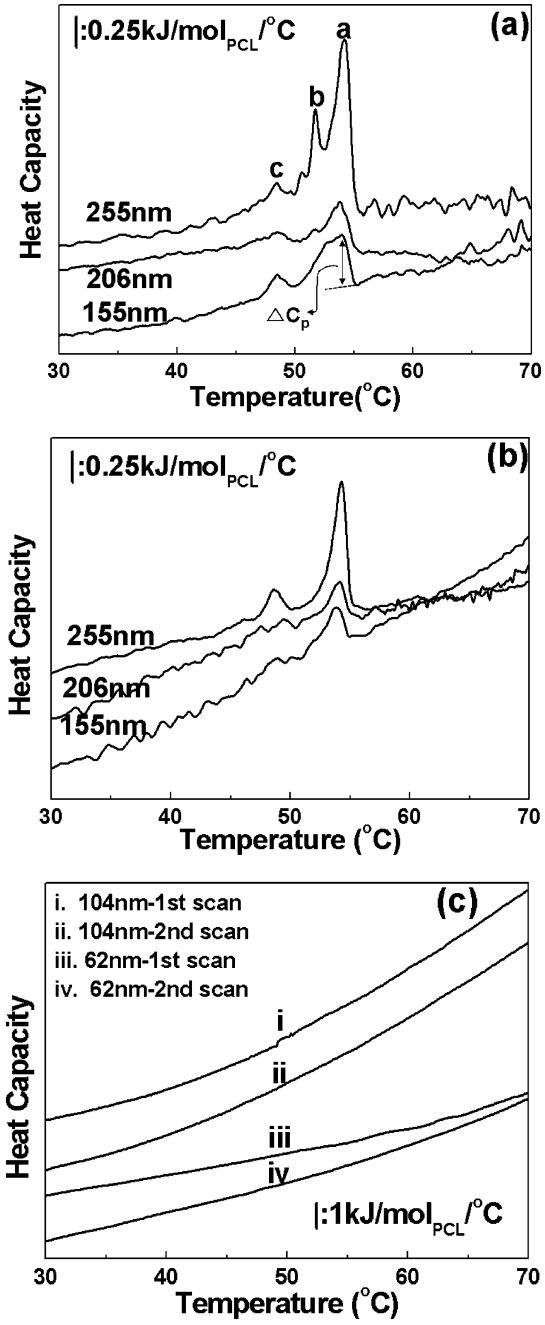

Figure 5. Microcalorimetry thermograms for PCL/PCL-*b*-PEO nanoparticle solutions: (a) first scan from 5 to 80 °C; (b) second scan from 5 to 80 °C after cooling from 80 to 5 °C for the particles of size 255, 206, and 155 nm. (c) shows the first and the second scans for the particles of size 104 and 62 nm.

Effect of the Block Copolymer on the Crystalline Structure of PCL/ PCL-*b*-PEO Nanoparticles. Another suggestion is that the PCL component in the PCL-*b*-PEO block copolymer does not participate in crystallization within the core. This can be proven by the fact that particles of sized 104 and 62 nm did not show any melting peak in the thermograms. Since hydrophilic PEO chains generally extend out from a nanoparticle toward the water phase, it is expected that PCL molecules linked to the PEO chains are not free to fold and are thus unable to form lamella structures. Figure 6 shows TEM micrographs of the PCL/PCL-*b*-PEO nanoparticles with sizes of 62 nm (Figure 6a,c) and 255 nm (Figure 6b,d). From Figure 6a, it can be seen that some of the particles (62 nm) are gathered together with many of the tails located outside of the particle (core). This

Table 2. Thermal Analysis of the PCL/PCL-*b*-PEO Nanoparticles

composn [PCL]/ [PCL-b-PEG]	av diameter (nm)	peak temp (°C) (first scan)			ΔC_p[b] at 54 °C (kJ/(mol/°C))	
		a[a]	b	c	first[c]	second
20	255	54.2	51.7	48.4	1.43	1.05
3	206	53.8	51.7	48.4	0.40	0.30
1	155	54.0	52.7[d]	48.4	0.39	0.28
0.33	104	*e*	*e*	*e*	*e*	*e*
0	62	*e*	*e*	*e*	*e*	*e*

[a] a−c represent the peak assigned in Figure 5a. [b] ΔC_p is the heat capacity difference between the peak around 54 °C and the baseline value at peak temperature (Figure 5a). [c] First and second indicates the first and second scan of the nanoparticle solutions. [d] Shoulder was detected. [e] Not detected.

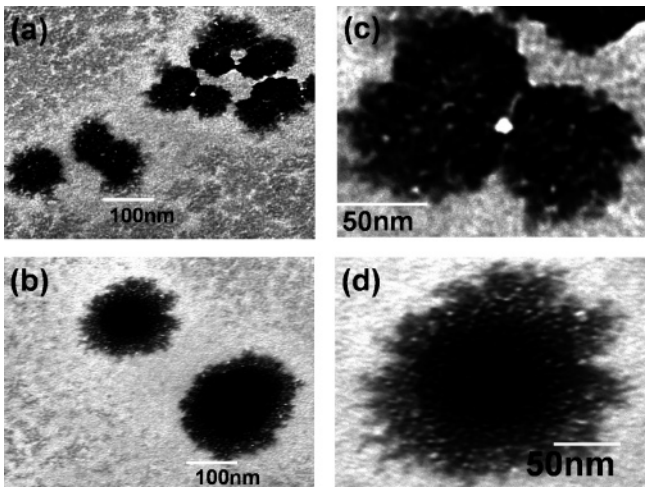

Figure 6. TEM micrographs for the nanoparticles of size (a) 62 nm and (b) 255 nm. (c) and (d) are magnified images of (a) and (b), respectively.

so-called core−shell (tail) structure can be clearly seen for the larger nanoparticles (255 nm) in Figure 6b. Since PEO is soluble in water, it is thought that the PEO chains in the block copolymer are "tailed" around the nanoparticle PCL "core". From the magnified images of Figure 6a,b, shown in Figure 6c,d respectively, it can be seen that the core structures of the two nanoparticles are different. For the smaller nanoparticles (62 nm), a number of holes can be seen in the nanoparticle cores that are not present in the larger nanoparticles (255 nm). These holes indicate that the nanoparticle core structure is not compact, providing further justification for why the thermograms of the 62 nm nanoparticles do not show a crystalline melting peak. Under these conditions, the PCL homopolymer could be only involved in the formation of crystalline domains in the PCL/PCL-*b*-PEO nanoparticles.

The possibility that the PCL in the block copolymer cannot crystallize in the PCL/PCL-*b*-PEO nanoparticle might also suggest that the blending of PCL homopolymer and amorphous PCL decrease the crystallinity of the PCL homopolymer. This suggestion is supported by the observed decrease in crystallinity of PCL in the miscible blended systems of PCL/poly(styrene-*co*-acrylonitrile) copolymer,[24] PCL/poly(vinyl chloride),[17] and PCL/starch.[25] In this respect, the observed decrease in ΔC_p with decreasing size is likely due to the increased amount of amorphous PCL in the PCL/PCL-*b*-PEO block copolymer, where amorphous PCL hinders crystallization of the PCL homopolymer.

The PCL homopolymer content in the PCL/PCL-*b*-PEO nanoparticles of size 206 and 155 nm is estimated at approximately 75% and 50%, respectively, as compared to the PCL content in the slightly larger nanoparticle (255 nm). However, the experimental ΔC_p values for these smaller nanoparticles are still lower than the ΔC_p values estimated from the remaining PCL homopolymer relative to the slightly larger nanoparticle (255 nm). The above estimation might support our ideas: the decreasing particle size and the blending of amorphous PCL with crystalline PCL further decreases the crystallinity of PCL in the nanoparticles.

Effect of Thermal Treatment on the Crystalline Structure of the PCL and PCL/PCL-*b*-PEO Nanoparticles. When one compares the thermograms of the PCL homopolymer nanoparticles (Figure 3) with those of the PCL/PCL-*b*-PEO nanoparticles (Figure 5 and Table 2), it can be seen that the heating and cooling of these nanoparticles caused different results. For the PCL homopolymer nanoparticles, like the bulk PCL (Figure 2a) and PCL microparticles,[7] it is thought that the annealing process causes PCL to crystallize, forming a more stable structure without significantly changing the crystallinity. In contrast, the ΔC_p value for the PCL/PCL-*b*-PEO nanoparticles decreased to ≈20−25% during the second scan (as compared with ΔC_p for the first scan), without a change in melting peak temperature. As in the case of the PCL homopolymer nanoparticles, the sizes of the PCL/PCL-*b*-PEO nanoparticles before and after the experiment have the same hydrodynamic diameters within experimental errors. Here, the same particle diameters were observed for these nanoparticles after annealing at 40, 50, and 60 °C.

The above results imply that some part of the crystalline core in the nanoparticles becomes disordered during the heating and cooling processes. One possible explanation that would account for this is that the PCL homopolymer and the PCL component in the block copolymer become more homogeneous as the temperature increases beyond the melting temperature of PCL. This homogeneous mixing of the two molecules might hinder PCL from recrystallizing during the cooling process, because the PCL chain in the block copolymer is not crystallizable (Figure 5 and Table 2) and thus might serve as a "defect site" during crystallization of the PCL homopolymer. This would result in a decrease in the ΔC_p for the second scan, as compared with the ΔC_p of the as-prepared PCL/PCL-*b*-PEO nanoparticles.

Conclusions

We have investigated the structure of semicrystalline nanoparticles by preparing two different types: PCL homopolymer nanoparticles and PCL/PCL-*b*-PEO nanoparticles. The two nanoparticles exhibited an identical melting peak temperature, and this temperature was ≈3−4 °C lower than the melting temperature of the bulk PCL. We did not observe any size-dependent melting temperature change for the two nanoparticle types. Instead, for the PCL/PCL-*b*-PEO nanoparticles, a part of the crystalline core was found to decrease as the particle size decreased. This result is thought to be due to that the noncrystallizable PCL in the block copolymer affects the decrease in the crystallinity of PCL nanoparticles and that the decrease in the size also affects the decrease in the crystalline region. Our results show that both PCL and PCL/PCL-*b*-PEO nanoparticles are influenced by thermal history, although this thermal effect produces different results for each of the two nanoparticles.

References and Notes

(1) Roy, K.; Mao, H.-Q.; Huang, S.-K.; Leong, K. W. *Nat. Med.* **1999**, *5*, 387−391. Panyam, J.; Labhasetwar, V. *Mol. Pharm.* **2004**, *1*, 77−84. Fu, J.; Li, X.; Ng, D. K. P.; Wu, C. *Langmuir* **2002**, *18*, 3843−3847. Bodnar, M.; Hartmann, J. F.; Borbely, J. *Biomacromolecules* **2005**, *6*, 2521−2527. Kallinteri, P.; Higgins, S.; Hutcheon, G. A.; St. Pourcain, C. B.; Garnett, M. C. *Biomacromolecules* **2005**, *6*,

1885−1894. Shenoy, D.; Little, S.; Langer, R.; Amiji, M. *Mol. Pharm.* **2005**, *2*, 357−366. Lynn, D. M.; Anderson, D. G.; Putnam, D.; Langer, R. *J. Am. Chem. Soc.* **2001**, *123*, 8155−8156. Dalhaimer, P.; Engler, A. J.; Parthasarathy, R.; Discher, D. E. *Biomacromolecules* **2004**, *5*, 1714−1719.

(2) Shim, J.; Kang, H. S.; Park, W.-S.; Han, S.-H.; Kim, J.; Chang, I.-S. *J. Controlled Release* **2004**, *97*, 477−484. Müller-Goymann, C. C. *Eur. J. Pharm. Biopharm.* **2004**, *58*, 343−356. Müller, R. H.; Radtke, M.; Wissing, S. A. *Adv. Drug Del. Rev.* **2002**, *54*, S131−S155.

(3) Horch, R. A.; Shahid, N.; Mistry, A. S.; Timmer, M. D.; Mikos, A. G.; Barron, A. R. *Biomacromolecules* **2004**, *5*, 1990−1998. Sahoo, S. K.; Panda, A. K.; Labhasetwar, V. *Biomacromolecules* **2005**, *6*, 1132−1139. Zhu, H.; Ji, J.; Tan, Q.; Barbosa, M. A.; Shen, J. *Biomacromolecules* **2003**, *4*, 378−386.

(4) Lee, J.; Cho, E. C.; Cho, K. *J. Controlled Release* **2004**, *94*, 323−335.

(5) Gillies, E. R.; Fréchet, J. M. J. *Bioconjugate Chem.* **2005**, *16*, 361−368. Padilla De Jesus, O. L.; Ihre, H. R.; Gagne, L.; Fréchet, J. M. J.; Szoka, F. C., Jr. *Bioconjugate Chem.* **2002**, *13*, 453−461. Gillies, E. R.; Fréchet J. M. J. *Drug Discovery Today* **2005**, *10*, 35−43. Ambade, A. V.; Savariar, E. N.; Thayumanavan, S. *Mol. Pharm.* **2005**, *2*, 264−272.

(6) Aliabadi, H. M.; Mahmud A.; Sharifabadi; A. D.; Lavasanifar, A. *J. Controlled Release* **2005**, *104*, 301−311.

(7) Jeong, J.-C.; Lee, J.; Cho, K. *J. Controlled Release* **2003**, *92*, 249−258.

(8) Chawla, J. S.; Amiji, M. M. *Int. J. Pharm.* **2002**, *249*, 127−138. Zhang, Q.; Clark, C. G., Jr.; Wang, M.; Remsen, E. E.; Wooley, K. L. *Nano Lett.* **2002**, *2*, 1051−1054.

(9) Xiong, X. Y.; Tam, K. C.; Gan, L. H. *J. Controlled Release* **2005**, *103*, 73−82. Zhang, Y.; Zhuo, R.-x. *Biomaterials* **2005**, *26*, 6736−6742.

(10) Bunjes, H.; Koch, M. H. J.; Westesen, K. *Langmuir* **2000**, *16*, 5234−5241.

(11) Castelli, F.; Puglia, C.; Sarpietro, M. G.; Rizza, L.; Bonina F. *Int. J. Pharm.* **2005**, *304*, 231−238.

(12) Kang, H. S.; Kwon, S.-S.; Nam, Y.-S.; Han, S.-H.; Chang, I.-S. *J. Colloid Interface Sci.* **2002**, *255*, 352−355.

(13) Grinberg, V. Y.; Dubovik, A. S.; Kuznetsov, D. V.; Grinberg, N. V.; Grosberg, A. Y.; Tanaka, T. *Macromolecules* **2000**, *33*, 8685−8692.

(14) . Privalov, P. L.; Gill, S. J. *Pure Appl. Chem.* **1989**, *61*, 1097.

(15) Kwon, S. S.; Nam, Y. S.; Lee, J. S.; Ku, B. S.; Han, S. H.; Lee, J. Y.; Chang, I. S. *Colloid Surf., A* **2002**, *210*, 95−104.

(16) Zweers, M. L. T.; Grijpma, D. W.; Engb. *J. Biomed. Mater. Res., B* **2003**, *66B*, 559−566. Konan, Y. N.; Gurny, R.; Allemann, E. *Int. J. Pharm.* **2002**, *233*, 239−252.

(17) Ong, C. J.; Price, F. P. *J. Polym. Sci. Polym. Symp.* **1978**, *63*, 45−58. Huarng, J. C.; Min, K.; White, J. L. *Polym. Eng. Sci.* **1988**, *28*, 1590−1599.

(18) Chatani, Y.; Okita, Y.; Tadokoro, H.; Yamashita, Y. *Polym. J.* **1970**, *1*, 555−562. Nishio, Y.; Manley, R. J. *Polym. Eng. Sci.* **1990**, *30*, 71−82.

(19) Wunderlich, B. *Macromolecular Physics, Crystal Nucleation, Growth, Annealing*; Academic Press: New York, 1976; Vol. 2, p 168.

(20) Westesen, K.; Bunjes, H. *Int. J. Pharm.* **1995**, *115*, 129−131.

(21) Westesen, K.; Siekmann, B.; Koch, M. H. J. *Int. J. Pharm.* **1993**, *93*, 189−199.

(22) Fukui, K.; Sumpter, B. G.; Barnes, M.; Noid, D. W. *Macromolecules* **2000**, *33*, 5982−5987.

(23) Wang, Y.; Ge, S.; Rafailovich, M.; Sokolov, J.; Zou, Y.; Ade, H.; Luning, J. Lustiger, A.; Maron, G. *Macromolecules* **2004**, *37*, 3319−3327.

(24) Rim, P. B.; Runt, J. P. *Macromolecules* **1983**, *16*, 762−768.

(25) Averous, L.; Moro, L.; Dole, P.; Fringant, C. *Polymer* **2000**, *41*, 4157−4167.

BM050883S